Journal of Water Process Engineering 34 (2020) 101078

Contents lists available at ScienceDirect

Journal of Water Process Engineering

journal homepage: www.elsevier.com/locate/jwpe

Low cost and quick time absorption of organic dye pollutants under ambient condition using partially exfoliated graphite

J. Mohanraj[a], D. Durgalakshmi[a,*], S. Balakumar[b], P. Aruna[a], S. Ganesan[a], Saravanan Rajendran[c], Mu. Naushad[d]

[a] Department of Medical Physics, Anna University, Chennai, India
[b] National Centre for Nanoscience and Nanotechnology, University of Madras, Chennai, India
[c] Faculty of Engineering, Department of Mechanical Engineering, University of Tarapaca, Avda. General Velasquez 1775, Arica, Chile
[d] Department of Chemistry, College of Science, Bld#5, King Saud University, Riyadh, Saudi Arabia

ARTICLE INFO

Keywords:
Corn cob
Partially exfoliated graphite
Adsorption
Methylene blue
Rhodamine B
Hydrogen evolution reaction

ABSTRACT

Worldwide, the removal of organic effluent dyes from domestic water is of high need due to the lesser availability of drinking water. In the present work, we reported on the synthesis of partially exfoliated graphite from corn cob and its ability to adsorb halogenated organic dyes. The synthesis of partially exfoliated graphene (PEG) showed the ability to adsorb the organic dyes at a quick time of about 5 s, even without any additional mechanical and radiation requirements. The adsorptive behavior of partially exfoliated graphite was conducted in an ambient condition, in the presence of halogenated organic dyes such as Methylene blue (MB) and Rhodamine B (RhB) as the adsorbate model. From the UV–vis absorption studies, it was observed that 1 mg of this sample had the efficiency to adsorb 0.1 mg/mL of MB and 0.01 mg/mL of RhB with the adsorption efficacy of 45 % and 75 %, respectively. The adsorption performance was well fitted with non-linear Gaussian regression plot for MB (R^2 = 0.9841) and RhB (R^2 = 0.7781).The photoluminescence studies also show that decreases in the intensity from the initial concentration of the MB and RhB dyes. The deconvoluted photoluminescence spectrum for both MB and Rh B showed peak broadening with peak shift for MB and the merged peaks for Rh B. The results suggested that, the partially exfoliated graphite can be utilized as an efficient low cost recyclable adsorbate for organic dye domestic effluent at low cost and also at a sustainable way. The partially exfoliated graphite also observed the possibility of hydrogen evolution reaction and opens the option of metal doping for futuristic applications.

1. Introduction

Organic dyes are widely used in the industries of pharmaceuticals, food, paper and pulp manufacturing; additives for plastics, dyeing of cloth, leather treatment and printing industries. During dying process, a large amount of dye has been mixed as effluent in domestic water bodies [1–4]. This caused lot of health issues such as skin irritation, contact dermatitis, permanent blindness, acute tubular necrosis supervene, vomiting gastritis, hypertension, vertigo and respiratory distress [5]. Some of these dyes are highly toxic to the environment as these highly concentrated colored dyes can inhibit the penetration of sunlight and oxygen, this in-turn alter the chemical oxygen demand (COD) and biochemical oxygen demand (BOD) values, essential for aquatic life [6]. In 2012 Rio Earth Summit, the topic of scarcity of non-contaminated water and growing need of drinking water was taken as one of the main issue need to be addressed at the earliest [7,8]. Worldwide, nearly 800,000 tons dyes were produced per year and out of this, about 10–15 % dyes are lost during processing in textile industry [9]. Removal of these kind of halogenated and non-halogenated dyes from industrial wastewater is very essential, but in most of the cases without neutralization it is often coming out in the form of an effluent and mixed with domestic water [10,11]. Hence, it is a very essential point to consider this issue from an environmental and economical concern. There are several approaches such as photocatalysis [12], thermal treatments and particulate based filtration, adsorption [13] etc. that led to eliminate these dyes mixing in domestic water [14]. Among these, adsorption is the versatile, efficient and cost effective methods for removal of these dyes from the wastewater effluents [15–17]. The dyes adsorbed by adsorption techniques also have the possibility to recycle and reuse for future applications. In general, most of the dyes are man-

* Corresponding author.
E-mail address: durgaklakshmi@gmail.com (D. Durgalakshmi).

https://doi.org/10.1016/j.jwpe.2019.101078
Received 30 September 2019; Received in revised form 10 November 2019; Accepted 16 November 2019
Available online 13 December 2019
2214-7144/ © 2019 Elsevier Ltd. All rights reserved.

made organic chemical contaminants [18], which includes halogenated, non-halogenated and pharmaceutical contaminants. The percentage of halogenated contaminants (e.g. Crystal violet, Eosin, Methylene blue, Safranin, Rhodamine B etc.) in textile effluents is higher compare to non-halogenated and pharmaceutical contaminants [19–24]

Conventionally, activated carbons are used for water purification for the particles in the range of 1 mm. Carbon based materials such as graphite, graphene, graphene oxide and carbon nanotubes are widely used in water purification due to its high surface area, ease of chemical or physical modification, excellent capacity for microbial disinfection and removal of both organic and inorganic contaminants [19,20,25–28]. Among these, carbons based materials, biomass derived graphene materials for removal of organic contaminants is less examined [29,30]. Some of the earlier reports on biomass include activated carbon production from corn cob [31], coconut shell/coir [32], rice husk [33,34], and wheat bran [35,36], used as sorbents for removal of water contaminates. The utilization of graphene based compounds from biomass paves a way to remove or denatures the particular contaminate at a cost effective technique [37–39].

Even though, lot of literature are reported on graphene oxide synthesized from graphite source for removal of contaminated dyes [40–44], very less paper has reported on the property of partially exfoliated graphite (PEG). Partially exfoliated graphite can be synthesized at lesser cost, lesser time and at higher yield compare to graphene oxide, which needs additional reducing conditions. Herein, we exemplified the possibilities of deriving partially exfoliated graphite corn cob. Worldwide each year more than 14 million metric tons of corn has been produced and the cob. However, it has been widely used for livestock with a limited application as manure and toilet papers after chemical modifications. The PEG obtained from corn cob has been employed to examine as a low cost absorbent for the removal of halogenated contaminant dye such as methylene blue(MB) and Rhodamine B (RhB).

2. Experimental techniques

2.1. Synthesis of partially exfoliated graphite

All the chemicals were purchased as an analytical grade and used without further purification. In-house prepared biochar of corn cob is used as source for synthesis of PEG. Hydrochloric acid (A.R grade), sulfuric acid (A.R grade), nitric acid (69 %), orthophosphoric acid (88 %), hydrogen peroxide (30 %), and potassium permanganate (98.5 %), were procured from Merck (U.S.A). Corn was collected from the farming land of Thiruvannamalai in India and was dried under sunlight. Once the kernels were dried, it was removed and the corn cob was sliced into thin pieces and washed with double distilled water to eliminate the adhered particulates. Dried corn shell of 35 g was sliced and washed thrice with double distilled to remove the impurities. Later it was dried overnight at 100 °C to remove the moisture and utilized to prepare graphite with a yielded of about 6 g.

In details, the washed and dried corn cob was pyrolized at 900ºC for three hours in the presence of N_2/Ar atmospheric to eliminate any organic polymers and the resultant will be the graphite biochar (Fig. 1a) [45]. This graphite was used for synthesis of PEG by improved Hummers method [46]. 100 mg graphite was taken in 10 mL of 1 M HNO_3 at 75°C and stirred for 1 h. The above mixture was then kept in an ice bath maintained at 10°C, followed slow addition of 0.3 g of $KMnO_4$and 12 mL of H_2SO_4 and this oxidizing reaction was allowed to happen for 30 min. Later 130 mL of H_3PO_4 was added and maintained at the temperature of 60°C for 24 h, this reaction was completed with addition of 100 mL of H_2O_2 quenching agent. The resultant PEG was washed with concentrated HCl to remove any unreacted compounds and wash with water until it reaches the pH 7 and dried at 120°C for 24 h. The PEG produced by this method has 75 % yield percentage which is very high compare to other chemical method of preparing graphene oxide. Other important advantages of this method are simple protocol, reduction of evolution of toxic gases during reaction and can able to synthesis at the commercial scale. Fig. 1 (b) shows a schematic representation of synthesis of partially exfoliated graphite from biochar.

2.2. Characterization techniques

Raman spectroscopy (LabRAM-laser wavelength-633 nm, France) was used to measure the formation of graphite and partially exfoliated graphite. FTIR spectra were recorded using FTIR spectroscopy (Jasco FT/IR -6600, U.S.A) in between 4000 to 400 cm^{-1} to confirm the functional groups in the graphite, and partially exfoliated graphene oxide. The morphology of the samples was observed using Scanning Electron Microscopy (Hitachi-N3400, Singapore). Prior to SEM analysis, the surface was coated with gold using ion sputtering technique about 7 s in order to obtain a secondary electron signal. Photoluminescence analysis was carried out using *Molecular devices-spetraMax* equipment and the PL spectra were deconvoluted using *fityk* software. Electrocatalytic studies were carried out using Cyclic Voltammetry (Biologic Instrument - SP 300, France).

2.3. Dye adsorption experiments

Adsorption studies for both methylene blue (MB) and Rhodamine B (RhB) dye were carried out by the addition of 1 mg of partially exfoliated graphene oxide to 2 mL of different concentration of dyes. The concentration of MB dyes was prepared with two different concentrations one is1 mg of dye in 10 mL of double distilled water and another in 5 mg of dye and Rhodamine B in 500 mL of double distilled water. For Rhodamine B, 5 mg dye was dissolved in 500 mL of double distilled water. The concentrations of dyes were measured using UV–vis spectroscopy at the wavelength of maximum absorbance intensity. The adsorption efficiency of the dye was calculated by the following equation [47,48]:

$$\text{adsorption efficiency R}\,(\%) = [\frac{(Co - C)}{Co}] \times 100$$

where Co and C denotes that the initial (before adsorption) and final (after adsorption) concentration of dyes in mg L^{-1}, respectively.

2.4. HER activity studies

To study on electrocatalysts, the sample ink was prepared in the ratio of 1:1:1 (water/isopropyl alcohol/Nafion) and then it was sonicated for 3 h. From this, 100 µL of prepared solution was added to prepare slurry into the presence of 5 mg of catalyst, which was again sonicated for 30 min. The prepared catalyst ink was then coated on the GCE and followed by that the modified electrode was allowed to dry it at room temperature. All the experiments were studied on the GCE in the presence of 1 M of H_2SO_4 solution using standard three electrode system at a slow scan rate 5 mV S^{-1} [49].

3. Results and discussions

3.1. Structural analysis

Raman spectroscopy is a sensitive fingerprint technique for the analysis of carbon and its derivate. Fig. 2(a) shows the Raman spectrum of graphite and PEG. The characteristic D and G bands for graphite are at 1324 cm^{-1} and 1597 cm^{-1} and for PEG the peaks are at 1340 cm^{-1} and 1593 cm^{-1}, respectively. The characteristic D band is attributed to the distortion of carbon structure or defect in layered graphite and the G band corresponds to ordered graphite layers. The relative Raman intensity I_D/I_G ratio for graphite and PEG are 1.2 (higher disorder/defect density), and 0.9, respectively. This indicates that compare to

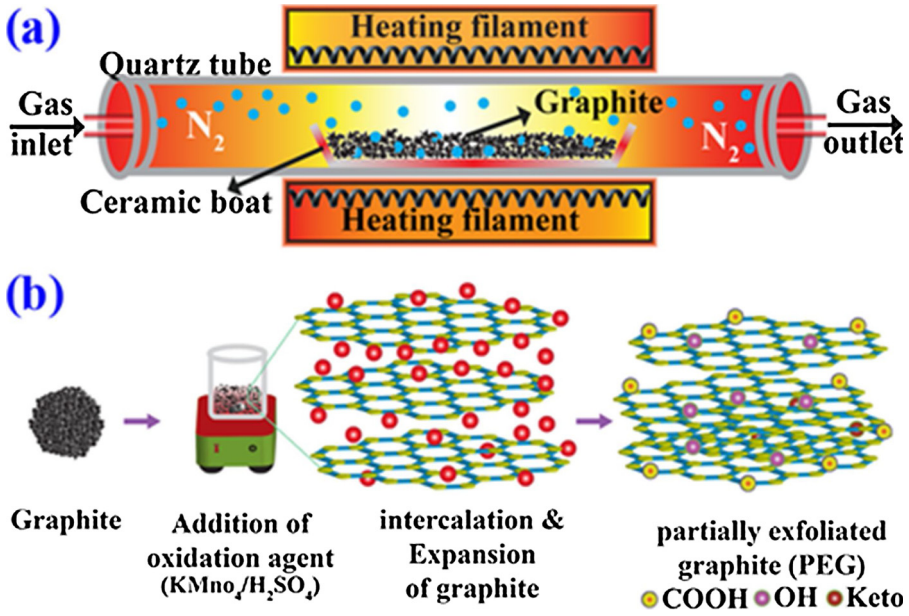

Fig. 1. Schematic representation of (a) Preparation of graphite from biomass and (b) Synthesis of PEG by improved hummers method.

graphite, PEG has graphitic nano sheets with increase in magnitude of graphitization by removal of functional group by exfoliation [50,51]

The typical XRD spectrum of graphite and PEG is shown in Fig. 2 (b), which indicates that graphite and PEG consists of microcrystalline graphite with hexagonal structure (JCPDS # 656212). It could be clearly shown there is two broad peaks at 21.8° and 43.7° for graphite and 23.7° and 42.3° for PEG, corresponding to (002) and (100) planes of graphene respectively [52]. There is a shift in the (002) plane peak around 2° towards higher degree depicts that compare to graphite, the exfoliated PEG shows well-arranged planner arrangement due to chemical and thermal treatments. The graphite peak is also showing lesser intensity compare to PEG and shows similar peak as graphene, due to the production of graphite from the biomass.

Fig. 2 (c) represents the FTIR spectrum of raw corn cob, graphite, and PEG. The raw corn cob spectrum has the band around 1628 cm^{-1} corresponds to the cellulose functional group. The next band approximately at 1601 cm^{-1}, 1523 cm^{-1}, and 1433 cm^{-1} refers to the aromatic skeletal vibration of lignin, followed by the band around 1322 cm^{-1}, 1245 cm^{-1}, 1154 cm^{-1} and 1032 cm^{-1} are the evidences of hemicellulose. The recorded band at 890 cm^{-1} corresponds to the β-(1→4) glycosidic bands between the xylose units in the hemicellulose [45,53]. The obtained graphite spectra possess quite a broad band around 1032 cm^{-1} to 1536 cm^{-1} is difficult to assign, owing to several superimposed peaks, the smaller peak at 1685 cm^{-1} is attributed to C=O vibration, corresponds to the carbonyls and carboxylic group. The synthesized PEG has higher intense peak around 1708 cm^{-1} and 1582 cm^{-1} compared with graphite, which is evidences, the presence of higher oxygen functional groups. The peak at 1572 cm^{-1} and 1712 cm^{-1} are attributed to C=C stretches with highly conjugated carboxyl groups and C=O stretching with conjugated aromatics, respectively [45,54].

3.2. Morphological studies

The SEM images of the raw corn, graphite, and partially exfoliated graphite is given in Fig. 3. The magnified surface of raw corn cob (Fig. 3a) shows wrinkled double gauze like structure. The thermal treated graphite surface has a porous structure (Fig. 3b). These porous structures were formed due to the evaporation of cellulose which was confirmed from FTIR and the breaking of carbon-carbon bond between the cellulose structures during pyrolysis. Fig. 3c confirms the formation of PEG from graphite biochar from the repetitious wrinkles on the surface. The elemental composition was confirmed from EDAX spectrum 3(e–f), which indicates that there exists only carbon in graphite and carbon with oxygen in PEG.

3.3. Dye adsorption studies

3.3.1. Adsorption of methylene blue dye

The adsorption of organic dye in the presence of PEG at various concentrations at room temperature was observed and given in Fig. 4. In this work, adsorbent (PEG) quantity was fixed as 1 mg/ 2 mL and the concentration of dyes (methylene blue and Rhodamine B) were varied. Generally, 10 mg/1 L (i.e. 0.02 mg/2 mL) concentration of dye was used

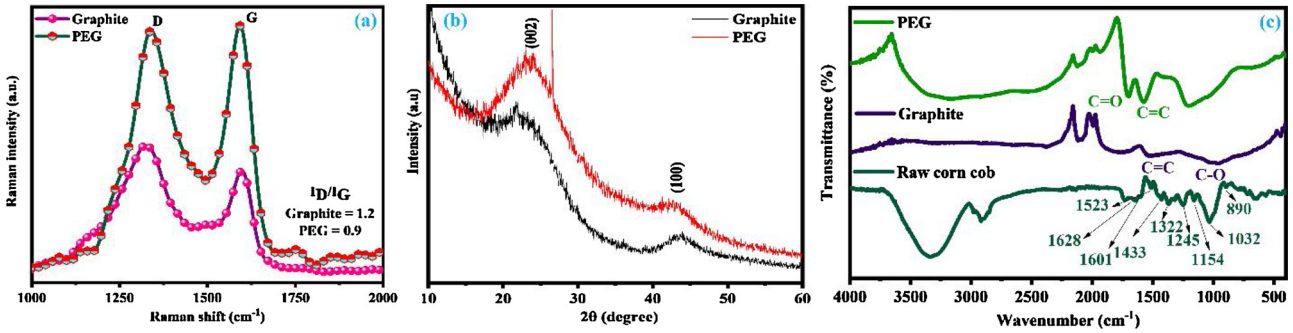

Fig. 2. (a) Raman spectrum, (b) XRD spectrum and (c) FTIR spectrum of graphite and PEG.

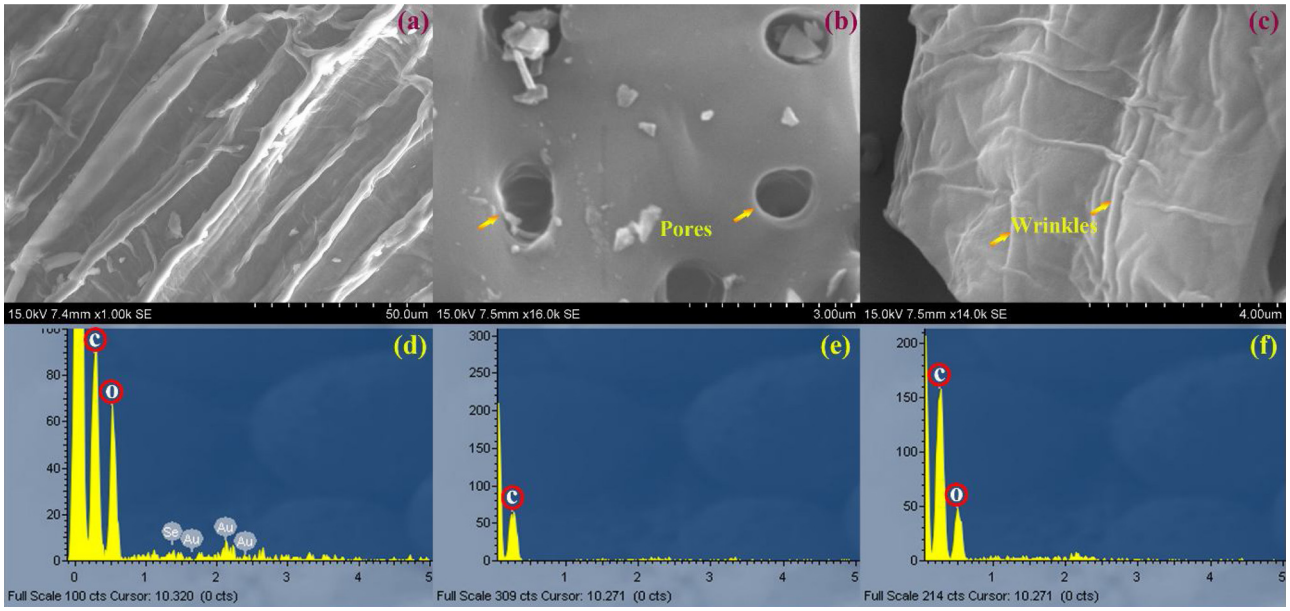

Fig. 3. SEM images of (a) raw corn cob, (b) graphite, (c) partially exfoliated graphene and their corresponding EDX represented in d to f.

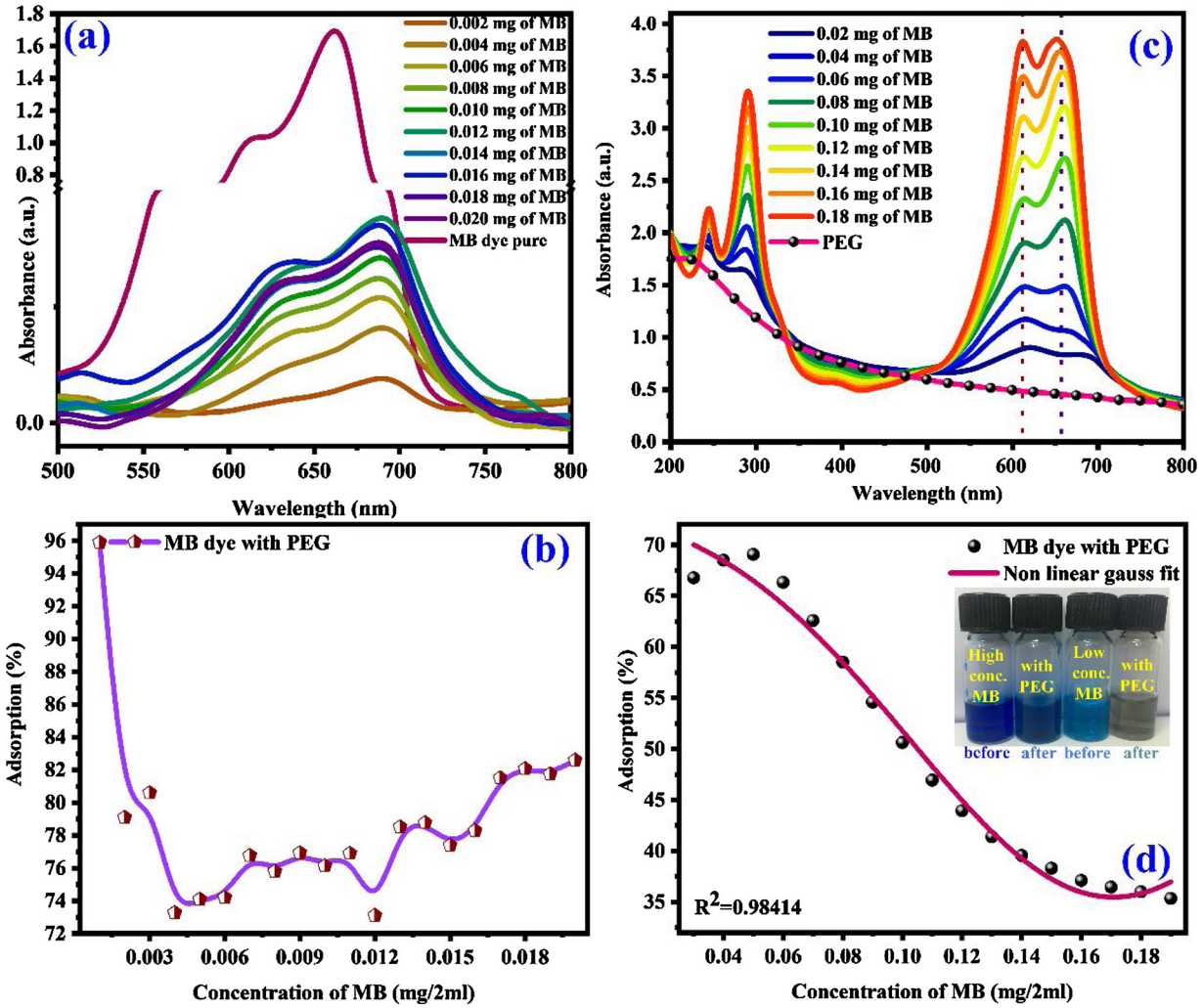

Fig. 4. UV–vis absorption spectrum (a) MB at low concentration(0.02 mg/2 mL) in the presence of PEG and its (b) absorption efficacy; (c) MB at higher concentration (0.19 mg/2 mL)in the presence of PEG and its (d) absorption efficacy (Inset: photograph of different concentration of MB along with PEG before and after adsorption).

in most of the literature for dye degradation studies [55–58]. The measured quantity of the dye was added in the presence of PEG and the UV spectra were observed at ambient condition. At lower concentration, there was visible absorption of dye with in few seconds (~ 5 s) and each reading with respect to the increasing in concentration was recorded and shown in Fig. 4a and c.

In order to compare our adsorption results with the degradation results of above mentioned concentration, adsorption gradient studies with fixed adsorbate (PEG) has been studied and given in Fig. 4a. The calculated adsorption efficacy for the standard dye concentration (10 mg/1 L) was found to be around 82 % (Fig. 4b), which is very high compare to the photocatalytic based degradation studies [59–61], that too within quick adsorption time and without any external photon/thermal activation. In order to observe the maximum adsorption efficacy of PEG, the concentration was increased 10 times from 0.04 mg/2 mLto 0.19 mg/2 mL and its absorbance spectra (Fig. 4c) was observed and its respective adsorption efficacy (Fig. 4d) has been calculated. Even for higher concentration for 0.19 mg/2 mL, the adsorption efficacy was found to be 35 %, which is very much higher compare to the earlier reports [59–61]. At higher concentration, the adsorption percentage reaches saturated due to accumulation of active sites in PEG by methylene blue dye.

3.3.2. Adsorption of rhodamine B

Similar to adsorption studies of low concentration of MB with PEG, RhB was taken at the standard concentration of 10 mg/1 L (i.e. 0.02 mg/2 mL), shown in Fig. 5. The adsorption of Rh B also occurred at quick time in ambient condition [Fig. 5a]. However, the adsorption percentage is lesser compare to MB. The maximum adsorption percentage for 0.02 mg/2 mL is 74 %, with the maximum adsorption percentage reaches around 80 % for low concentration of dyes, shown in Fig. 5b. Even though the difference in the adsorption activity between these two dyes is only around 1.1 %, this small difference could be due to the interaction of the dyes with the PEG active sites.

3.3.3. Photoluminescence studies of PEG with organic dyes

The photoluminescence emission spectra of MB dye (0.02 mg/2 mL), MB dye (0.02 mg/2 mL) with PEG and MB dye (0.19 mg/2 mL) excited at λ = 625 nm is given in Fig. 6. The emission spectra were observed to be at 695 nm and 705 nm for pure MB and higher concentration of MB with PEG, respectively. There is feeble emission peak for lower concentration MB is observed compare to pure and higher concentration of MB with PEG. Further, the deconvolution photoluminescence emission spectra of MB and MB (higher conc.) with PEG has shown two peaks with the $\chi^2 = 1$. For MB, the maximum energy of the fitted peaks is at the region of 1.74 eV and 1.79 eV, for MB with PEG, the peak values are at 1.73 eV and 1.78 eV. This shows that the peaks are narrowed at higher concentration with shift in the energy level. The photoluminescence emission spectra of Rh B and Rh B with PEG, excitation at λ = 520nmis given in Fig. 7. The decreases in the emission intensity of RhB in presence of PEG can be easily compared that of the earlier adsorption studies. The deconvoluted spectra of pure Rh B consist of seven peaks, whereas for Rh B with PEG it shows only three peaks with the maximum energy at 2.15 eV, 2.06 eV and 1.95 eV. The decrease in the number of peaks may be due to the merging of peaks at lower intensity with peak broadening compare to the pure dye.

3.3.4. FTIR analysis of organic dye with PEG

Fig. 8a shows the FTIR spectrum of MB dye and MB with PEG. For pure MB, the band around 2809 cm^{-1} and 2715 cm^{-1} corresponds to the stretching vibration of −CH aromatic and $-CH_3$ methyl group, respectively. Further, the band at 1607 cm^{-1} to 1351 cm^{-1} attributed to the aromatic ring stretching in MB and the band corresponding to the C=C skeleton of the aromatic ring were obtained at 1171 cm^{-1} [62]. For Rh B, the bands at 1594 cm^{-1}, 1414 cm^{-1}, 1395 cm^{-1} and 928 cm^{-1} confirms the presences of C=C aromatic, $-CH_3$, C=N, and C−H aromatic vibrations respectively. The absorption band around 1740 cm^{-1} and 1054 cm^{-1} ascribed to antisymmetric vibrations of carboxylic (−COOH) group, and stretching vibrations of oxygen contain alkoxy C−O group, respectively, is given in Fig. 8b [47]. After adsorption of both the dyes by PEG, there is no variation in the band position of the dye molecule, which confirms that the molecule does not degrade in the presence of PEG and which can be utilized for further recycling process.

3.4. Hydrogen evaluation studies (HER)

The HER catalytic studies carried out for the graphite and partially exfoliated graphite is shown in the Fig. 9. The LSV curves (Fig. 9a) of graphite and PEG showed an onset potential of -0.44 V and -0.59 V, respectively. The comparison of HER activity with earlier reports is given in Table 1.

The possible hydrogen evolution reaction mechanism is a combination of the following reactions as follows,

Reaction mechanism I: Volmer reaction: $H_3O^+ + e^- \rightarrow H_{ads} + H_2O$

Heyrovsky reaction: $H_{ads} + H_3O^+ \rightarrow H_2 + H_2O$

Reaction mechanism II: Tafel reaction: $H_{ads} + H_{ads} \rightarrow H_2$

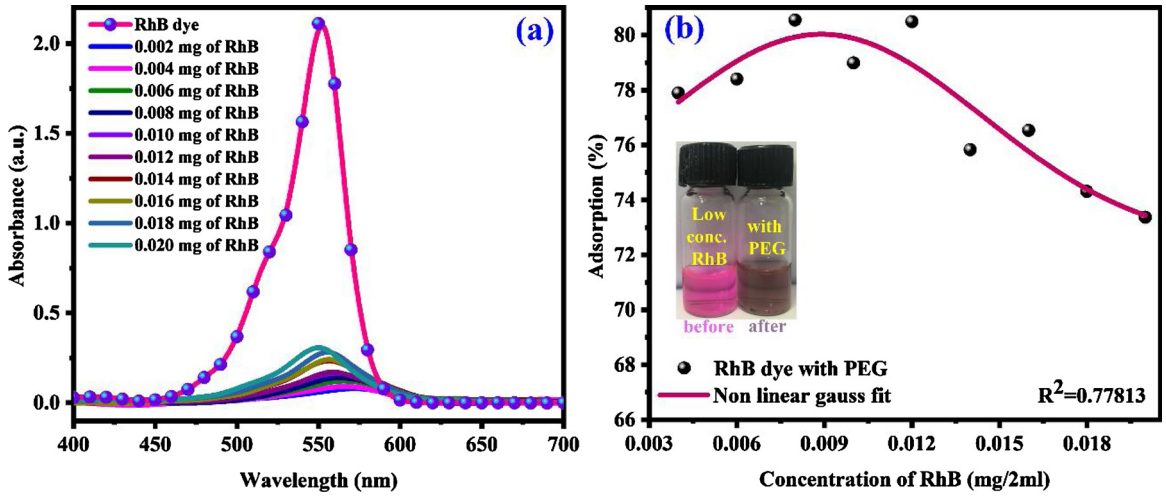

Fig. 5. UV–vis absorption spectrum (a) Rh B in the presence of PEG and its (b) absorption efficacy (Inset: photograph of lower concentration of RhB along with PEG before and after adsorption).

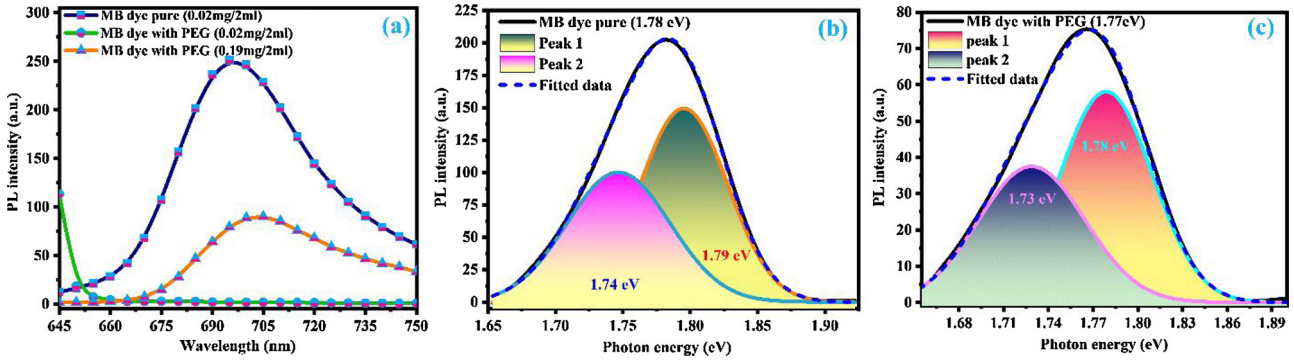

Fig. 6. Photoluminescence emission spectra (excitation at 625 nm) of (a) MB with PEG at different concentration, (b) deconvolution spectra of MB (0.02 mg/2 mL), and (c) deconvolution spectra of MB (0.19 mg/2 mL) with PEG.

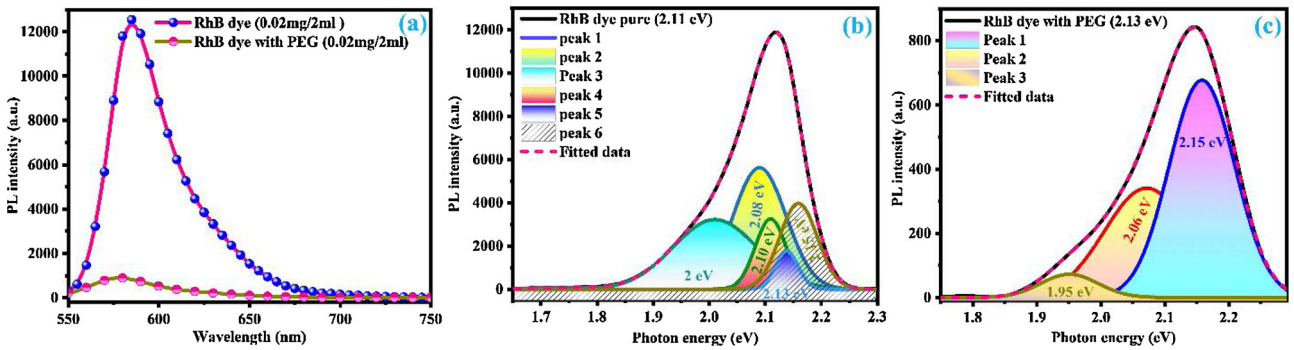

Fig. 7. Photoluminescence emission spectra (excitation at 520 nm) of (a) Rh B with PEG at different concentration, (b) deconvolution spectra of RhB (0.02 mg/2 mL) and (c) deconvolution spectra of Rh B (0.02 mg/2 mL) with PEG.

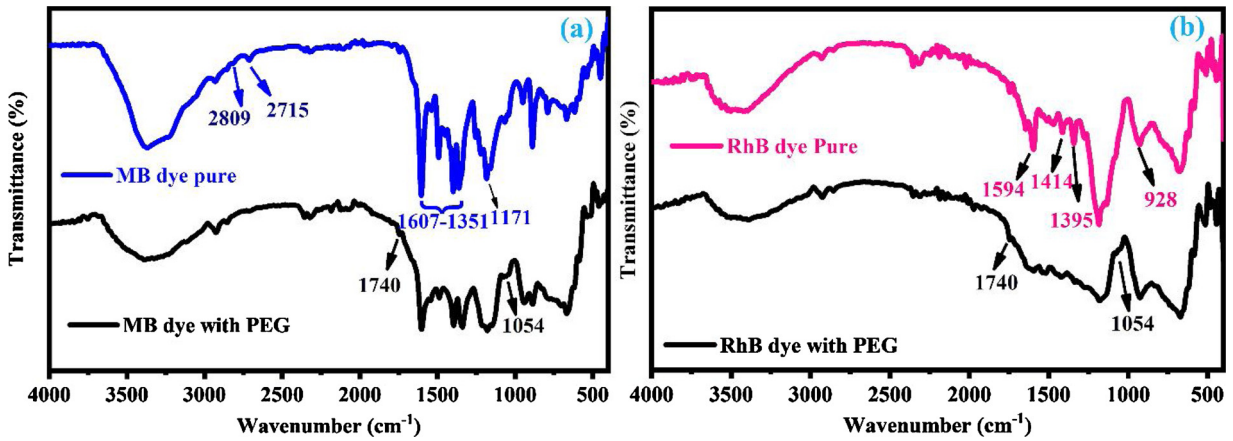

Fig. 8. FTIR spectra for (a) MB with PEG and (b) Rh B with PEG.

The fitted Tafel plot of graphite and PEG with the Tafel equation, n = a + b log j (where 'a' is the constant, b is the Tafel slope and j is the current density) is given in Fig. 9b. The obtained Tafel slopes are296 mV/dec and 153 mV/dec for the graphite and PEG, respectively. From this, the calculated over potential was 482 mV and 269 mV for the graphite and PEG, respectively. Hence from these results it is observed that, PEG samples have faster catalytic rate and evidenced for higher HER activity compared to graphite. During the electrochemical performance, in PEG, owing to the nano regime size effect it provides higher active surface sites and hence there is an occurrence of unexpectedly continuous hydrogen evolution reaction [26].

4. Conclusion

This work explores the new possibilities of low cost partially exfoliated graphite prepared from biomass corncob using improved Hummers method at a higher yield. The prepared partially exfoliated graphite also showed a potential ability as a cost effective adsorbent for the removal of halogenated organic dyes from domestic effluents without additional radiation. The prepared PEG adsorbent showed the excellent adsorbate efficiency of both dyes in water even in at higher concentration. From the FTIR results, it was concluded that the dye was absorbed without any functional damage and hence opens the venture for the further extraction of dye from PEG by proper chemical methods and can reuse for useful applications. The photoluminescence studies of dye and dye with adsorbate was observed with respect to energy variation for the first time. The prepared PEG also opens the other possibility of utilizing as hydrogen generation by suitable combination with metal ions in future.

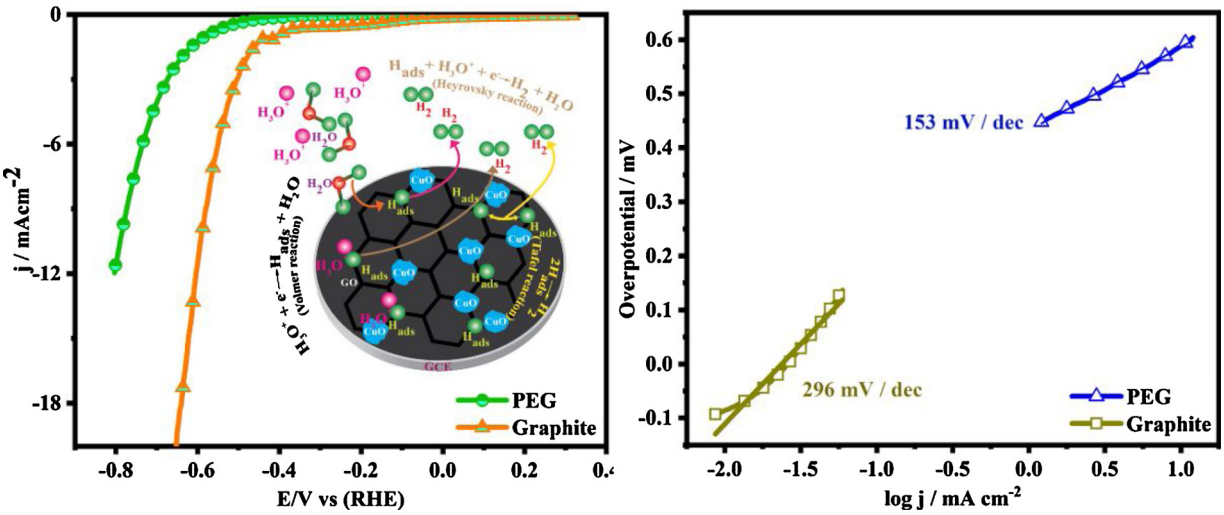

Fig. 9. Shows the (a) LSV curve and (b) Tafel plot.

Table 1
Comparison of the HER activity of this work with earlier reports.

S.No	Electrode	Overpotential (mV)	Tafel slop (mV/dec)	Ref.
1.	Cu_2SnS_3, Cu_4SnS_4	330, 358	98,110	[63]
2.	CuS/Au	449	171	[64]
3.	NiS	560	182	[65]
4.	DAC/MoS_2	332	−84	[66]
5.	Graphite, PEG	482, 269	296, 153	This work

Declaration of Competing Interest

The authors declare that there are no conflicts of interest regarding the publication of this paper.

Acknowledgements

The authors D. Durgalakshmi and J. Mohanraj gratefully acknowledges DST-INSPIRE Faculty Fellowship under the sanction DST/INSPIRE/04/2016/000845 for their funding. All the authors acknowledge DAE-BRNS - 2009/34/38/BRNS and DST-PURSE-9500/PD2/2014 for providing equipment facilities. R. Saravanangratefully acknowledges financial support from the SERC (CONICYT/FONDAP/15110019), and FONDECYT, Government of Chile (Project No.: 11170414). One of the authors (Mu. Naushad) acknowledge the Researchers Supporting Project number (RSP-2019/8), King Saud University, Riyadh, Saudi Arabia for the support.

References

[1] N.H.H. Hairom, A.W. Mohammad, A.A.H. Kadhum, Nanofiltration of hazardous Congo red dye: performance and flux decline analysis, J. Water Process Eng. 4 (2014) 99–106, https://doi.org/10.1016/j.jwpe.2014.09.008.
[2] A.A. Alqadami, M. Naushad, Z.A. Alothman, T. Ahamad, Adsorptive performance of MOF nanocomposite for methylene blue and malachite green dyes: kinetics, isotherm and mechanism, J. Environ. Manage. 223 (2018) 29–36, https://doi.org/10.1016/j.jenvman.2018.05.090.
[3] M.M. Ayad, A.A. El-Nasr, Adsorption of cationic dye (methylene blue) from water using polyaniline nanotubes base, J. Phys. Chem. C 114 (34) (2010) 14377–14383, https://doi.org/10.1021/jp103780w.
[4] N.H.H. Hairom, A.W. Mohammad, A.A.H. Kadhum, Influence of zinc oxide nanoparticles in the nanofiltration of hazardous Congo red dyes, Chem. Eng. J. 260 (2015) 907–915, https://doi.org/10.1016/j.cej.2014.08.068.
[5] B.J. Cardinale, J.E. Duffy, A. Gonzalez, D.U. Hooper, C. Perrings, P. Venail, A. Narwani, G.M. Mace, D. Tilman, D.A. Wardle, Biodiversity loss and its impact on humanity, Nature 486 (7401) (2012) 59, https://doi.org/10.1038/nature11148.
[6] L. Cheng, H. Liu, Y. Cui, N. Xue, W. Ding, Direct conversion of corn cob to formic and acetic acids over nano oxide catalysts, J. Energy Chem. 23 (1) (2014) 43–49, https://doi.org/10.1016/S2095-4956(14)60116-9.
[7] G.L. Dotto, J.M.d. Moura, T.R.S. Cadaval, L.A.A. Pinto, Application of chitosan films for the removal of food dyes from aqueous solutions by adsorption, Chem. Eng. 214 (2013) 8–16, https://doi.org/10.1016/j.cej.2012.10.027.
[8] M.P. Elizalde-González, Development of non-carbonised natural adsorbents for removal of textile dyes, Trends Chem. Eng. 10 (2006) 55–66 https://www.researchgate.net/profile/Maria_Elizalde-Gonzalez/publication/269038921_Development_of_non-carbonised_natural_adsorbents_for_removal_of_textile_dyes/links/5480678b0cf2ccc7f8bcec96/Development-of-non-carbonised-natural-adsorbents-for-removal-of-textile-dyes.pdf.
[9] M.P. Elizalde-González, J. Mattusch, R. Wennrich, Chemically modified maize cobs waste with enhanced adsorption properties upon methyl orange and arsenic, Bioresour. Technol. 99 (11) (2008) 5134–5139, https://doi.org/10.1016/j.biortech.2007.09.023.
[10] M. Naushad, A. Mittal, M. Rathore, V. Gupta, Ion-exchange kinetic studies for Cd (II), Co (II), Cu (II), and Pb (II) metal ions over a composite cation exchanger, Desalin. Water Treat. 54 (10) (2015) 2883–2890, https://doi.org/10.1080/19443994.2014.904823.
[11] M. Naushad, T. Ahamad, G. Sharma, A.H. Al-Muhtaseb, A.B. Albadarin, M.M. Alam, Z.A. ALOthman, S.M. Alshehri, A.A. Ghfar, Synthesis and characterization of a new starch/SnO2 nanocomposite for efficient adsorption of toxic Hg2+ metal ion, Chem. Eng. J. 300 (2016) 306–316, https://doi.org/10.1016/j.cej.2016.04.084.
[12] M. Naushad, G. Sharma, Z.A. Alothman, Photodegradation of toxic dye using Gum Arabic-crosslinked-poly (acrylamide)/Ni (OH) 2/FeOOH nanocomposites hydrogel, J. Clean. Prod. 241 (2019) 118263, , https://doi.org/10.1016/j.jclepro.2019.118263.
[13] M. Naushad, Z.A. ALOthman, Separation of toxic Pb2+ metal from aqueous solution using strongly acidic cation-exchange resin: analytical applications for the removal of metal ions from pharmaceutical formulation, Desalin. Water Treat. 53 (8) (2015) 2158–2166, https://doi.org/10.1080/19443994.2013.862744.
[14] T. Tatarchuk, N. Paliychuk, R.B. Bitra, A. Shyichuk, M. Naushad, I. Mironyuk, D. Ziółkowska, Adsorptive removal of toxic Methylene Blue and Acid Orange 7 dyes from aqueous medium using cobalt-zinc ferrite nanoadsorbents, Desalin. Water Treat. 150 (2019) 374–385, https://doi.org/10.5004/dwt.2019.23751.
[15] S. Khadivi, L. Edjlali, A. Akbarzadeh, K.J. Seyyedi, Enhanced adsorption behavior of amended EDTA–graphene oxide for methylene blue and heavy metal ions, Int. J. Environ. Sci. Technol. (2019) 1–10, https://doi.org/10.1007/s13762-019-02286-7.
[16] J.-Y. Mei, P. Qi, X.-N. Wei, X.-C. Zheng, Q. Wang, X.-X. Guan, Assembly and enhanced elimination performance of 3D graphene aerogel-zinc oxide hybrids for methylene blue dye in water, J. Mater. Res. Bull. 109 (2019) 141–148, https://doi.org/10.1016/j.materresbull.2018.09.034.
[17] J.-J. Zhang, S.-S. Fang, J.-Y. Mei, G.-P. Zheng, X.-C. Zheng, X.-X. Guan, High-efficiency removal of rhodamine B dye in water using g-C3N4 and TiO2 co-hybridized 3D graphene aerogel composites, J. Sep. Purf. Technol. 194 (2018) 96–103, https://doi.org/10.1016/j.seppur.2017.11.035.
[18] M. Naushad, Z.A. Alothman, M. Rabiul Awual, S.M. Alfadul, T. Ahamad, Adsorption of rose Bengal dye from aqueous solution by amberlite Ira-938 resin: kinetics, isotherms, and thermodynamic studies, Desalin. Water Treat. 57 (29) (2016) 13527–13533, https://doi.org/10.1080/19443994.2015.1060169.
[19] Y. Liu, M. Zhu, M. Chen, L. Ma, B. Yang, L. Li, W. Tu, A polydopamine-modified reduced graphene oxide (RGO)/MOFs nanocomposite with fast rejection capacity for organic dye, J. Chem. Eng. Sci. 359 (2019) 47–57, https://doi.org/10.1016/j.cej.2018.11.105.
[20] Y. Yang, W. Yu, S. He, S. Yu, Y. Chen, L. Lu, Z. Shu, H. Cui, Y. Zhang, H.J. Jin, Rapid adsorption of cationic dye-methylene blue on the modified montmorillonite/graphene oxide composites, Appl. Clay Sci. 168 (2019) 304–311, https://doi.org/10.1016/j.clay.2018.11.013.
[21] J. Han, B.-M. Jun, J. Heo, G. Lee, Y. Yoon, C.M.J. Park, Highly efficient organic dye removal from waters by magnetically recoverable La2O2CO3/ZnFe2O4-reduced

graphene oxide nanohybrid, Ceram. Int. (2019), https://doi.org/10.1016/j.ceramint.2019.06.173.
[22] A.Y. Sham, S.M.J. Notley, Adsorption of organic dyes from aqueous solutions using surfactant exfoliated graphene, J. Environ. Chem. Eng. 6 (1) (2018) 495–504, https://doi.org/10.1016/j.jece.2017.12.028.
[23] T.R. Das, S. Patra, R. Madhuri, P.K. Sharma, Bismuth oxide decorated graphene oxide nanocomposites synthesized via sonochemical assisted hydrothermal method for adsorption of cationic organic dyes, J. Collid. Interface. Sci. 509 (2018) 82–93, https://doi.org/10.1016/j.jcis.2017.08.102.
[24] J. Su, S. He, Z. Zhao, X. Liu, H. Li, Efficient preparation of cetyltrimethylammonium bromide-graphene oxide composite and its adsorption of Congo red from aqueous solutions, Collids Surf. A 554 (2018) 227–236, https://doi.org/10.1016/j.colsurfa.2018.06.048.
[25] M. Genovese, J. Jiang, K. Lian, N. Holm, High capacitive performance of exfoliated biochar nanosheets from biomass waste corn cob, J. Mater. Chem. A 3 (6) (2015) 2903–2913, https://doi.org/10.1039/C4TA06110A.
[26] J.A. González, M.E. Villanueva, L.L. Piehl, G.J. Copello, Development of a chitin/graphene oxide hybrid composite for the removal of pollutant dyes: adsorption and desorption study, Chem. Eng. 280 (2015) 41–48, https://doi.org/10.1016/j.cej.2015.05.112.
[27] M.A. Hassaan, A. El Nemr, Health and environmental impacts of dyes: mini review, Am. J. Environ. Sci. Eng. 1 (3) (2017) 64–67, https://doi.org/10.11648/j.ajese.20170103.11.
[28] K. Sartova, E. Omurzak, G. Kambarova, I. Dzhumaev, B. Borkoev, Z.J.D. Abdullaeva, Activated carbon obtained from the cotton processing wastes, Diam. Relat. Mater. 91 (2019) 90–97, https://doi.org/10.1016/j.diamond.2018.11.011.
[29] K. Gupta, D. Gupta, O.P. Khatri, Graphene-like porous carbon nanostructure from Bengal gram bean husk and its application for fast and efficient adsorption of organic dyes, Appl. Surf. Sci. 476 (2019) 647–657, https://doi.org/10.1016/j.apsusc.2019.01.138.
[30] G. Sharma, A. Kumar, S. Sharma, S.I. Al-Saeedi, G.M. Al-Senani, A. Nafady, T. Ahamad, M. Naushad, F.J. Stadler, Fabrication of oxidized graphite supported La_2O_3/ZrO_2 nanocomposite for the photoremediation of toxic fast green dye, J. Mol. Liq. 277 (2019) 738–748, https://doi.org/10.1016/j.molliq.2018.12.126.
[31] I. Hod, P. Deria, W. Bury, J.E. Mondloch, C.-W. Kung, M. So, M.D. Sampson, A.W. Peters, C.P. Kubiak, O.K. Farha, A porous proton-relaying metal-organic framework material that accelerates electrochemical hydrogen evolution, Nat. Commun. 6 (2015) 8304, https://doi.org/10.1038/ncomms9304.
[32] M. Karnan, K. Subramani, P. Srividhya, M. Sathish, Electrochemical studies on corncob derived activated porous carbon for supercapacitors application in aqueous and non-aqueous electrolytes, Electrochim. Acta 228 (2017) 586–596, https://doi.org/10.1016/j.electacta.2017.01.095.
[33] Y.-Y. Lau, Y.-S. Wong, T.-T. Teng, N. Morad, M. Rafatullah, S.-A. Ong, Degradation of cationic and anionic dyes in coagulation–flocculation process using bi-functionalized silica hybrid with aluminum-ferric as auxiliary agent, RSC Adv. 5 (43) (2015) 34206–34215, https://doi.org/10.1039/C5RA01346A.
[34] Y. Li, Q. Du, T. Liu, X. Peng, J. Wang, J. Sun, Y. Wang, S. Wu, Z. Wang, Y. Xia, Comparative study of methylene blue dye adsorption onto activated carbon, graphene oxide, and carbon nanotubes, Chem. Eng. Res. Des. 91 (2) (2013) 361–368, https://doi.org/10.1016/j.cherd.2012.07.007.
[35] F. Liu, S. Chung, G. Oh, T.S. Seo, Three-dimensional graphene oxide nanostructure for fast and efficient water-soluble dye removal, ACS Appl. Mater. Interfaces 4 (2) (2012) 922–927, https://doi.org/10.1021/am201590z.
[36] T. Madrakian, A. Afkhami, M. Ahmadi, Adsorption and kinetic studies of seven different organic dyes onto magnetite nanoparticles loaded tea waste and removal of them from wastewater samples, Spectrochim. Acta A 99 (2012) 102–109, https://doi.org/10.1016/j.saa.2012.09.025.
[37] M. Ghasemi, M. Naushad, N. Ghasemi, Y. Khosravi-Fard, Adsorption of Pb (II) from aqueous solution using new adsorbents prepared from agricultural waste: adsorption isotherm and kinetic studies, J. Ind. Eng. Chem. 20 (4) (2014) 2193–2199, https://doi.org/10.1016/j.jiec.2013.09.050.
[38] G. Sharma, M. Naushad, D. Pathania, A. Mittal, G.E. El-Desoky, Modification of Hibiscus cannabinus fiber by graft copolymerization: application for dye removal, Desalin. Water Treat. 54 (11) (2015) 3114–3121, https://doi.org/10.1080/19443994.2014.904822.
[39] G. Sharma, S. Sharma, A. Kumar, M. Naushad, B. Du, T. Ahamad, A.A. Ghfar, A.A. Alqadami, F.J. Stadler, Honeycomb structured activated carbon synthesized from Pinus roxburghii cone as effective bioadsorbent for toxic malachite green dye, J. Water Process Eng. 32 (2019) 100931, , https://doi.org/10.1016/j.jwpe.2019.100931.
[40] V. Maheskumar, P. Gnanaprakasam, T. Selvaraju, B. Vidhya, Comparative studies on the electrocatalytic hydrogen evolution property of Cu2SnS3 and Cu4SnS4 ternary alloys prepared by solvothermal method, Int. J. Hydrogen Energy 43 (8) (2018) 3967–3975, https://doi.org/10.1016/j.ijhydene.2017.07.194.
[41] D.C. Marcano, D.V. Kosynkin, J.M. Berlin, A. Sinitskii, Z. Sun, A. Slesarev, L.B. Alemany, W. Lu, J.M. Tour, Improved synthesis of graphene oxide, ACS Nano 4 (8) (2010) 4806–4814, https://doi.org/10.1021/nn1006368.
[42] M. Mostafa, Waste water treatment in textile Industries-the concept and current removal technologies, J. Biodivers. Environ. Sci. 7 (1) (2015) 501–525 https://www.researchgate.net/profile/Dr_Mostafa2/publication/303453038_Waste_water_treatment_in_Textile_Industriesthe_concept_and_current_removal_Technologies/links/574425d408ae9f741b3a2866.pdf.
[43] F. Perreault, A.F. De Faria, M. Elimelech, Environmental applications of graphene-based nanomaterials, Chem. Soc. Rev. 44 (16) (2015) 5861–5896, https://doi.org/10.1039/C5CS00021A.
[44] Y. Wu, F. Yang, X. Liu, G. Tan, D.J. Xiao, Fabrication of N, P-codoped reduced graphene oxide and its application for organic dye removal, Appl. Surf. Sci. 435 (2018) 281–289, https://doi.org/10.1016/j.apsusc.2017.10.118.
[45] G. Ramesha, A.V. Kumara, H. Muralidhara, S. Sampath, Graphene and graphene oxide as effective adsorbents toward anionic and cationic dyes, J. Colloid Interface Sci. 361 (1) (2011) 270–277, https://doi.org/10.1016/j.jcis.2011.05.050.
[46] D. Sangeetha, M. Selvakumar, Active-defective activated carbon/MoS 2 composites for supercapacitor and hydrogen evolution reactions, Appl. Surf. Sci. 453 (2018) 132–140, https://doi.org/10.1016/j.apsusc.2018.05.033.
[47] J. Tollefson, N. Gilbert, Earth summit: rio report card, Nat. News 486 (7401) (2012) 20, https://doi.org/10.1038/486020a.
[48] H. Zhao, X. Song, H.J. Zeng, 3D white graphene foam scavengers: vesicant-assisted foaming boosts the gram-level yield and forms hierarchical pores for superstrong pollutant removal applications, NPG Asia Mater. 7 (3) (2015) e168, https://doi.org/10.1038/am.2015.8.
[49] M. Shaban, M.R. Abukhadra, A. Hamd, R.R. Amin, A.A. Khalek, Photocatalytic removal of Congo red dye using MCM-48/Ni2O3 composite synthesized based on silica gel extracted from rice husk ash; fabrication and application, J. Environ. Manage. 204 (2017) 189–199, https://doi.org/10.1016/j.jenvman.2017.08.048.
[50] C. Ruan, K. Ai, L.J.R.A. Lu, Biomass-derived carbon materials for high-performance supercapacitor electrodes, Sustain. Energy Fuels. 4 (58) (2014) 30887–30895, https://doi.org/10.1039/C4RA04470C.
[51] W. Kang, B. Lin, G. Huang, C. Zhang, Y. Yao, W. Hou, B. Xu, B.J. Xing, Peanut bran derived hierarchical porous carbon for supercapacitor, J. Mater. Sci-Mater. Electron. 29 (8) (2018) 6361–6368, https://doi.org/10.1007/s10854-018-8615-1.
[52] Z. Shahryari, A.S. Goharrizi, M. Azadi, Experimental study of methylene blue adsorption from aqueous solutions onto carbon nano tubes, Int. J. Water Res. 2147483647 (2) (2010) 016–028 DOI:10.5897/IJWREE.
[53] Y.C. Sharma, S.N. Upadhyay, Removal of a cationic dye from wastewaters by adsorption on activated carbon developed from coconut coir, Energy Fuel. 23 (6) (2009) 2983–2988, https://doi.org/10.1021/ef9001132.
[54] S.C. Smith, D.F. Rodrigues, Carbon-based nanomaterials for removal of chemical and biological contaminants from water: a review of mechanisms and applications, Carbon 91 (2015) 122–143, https://doi.org/10.1016/j.carbon.2015.04.043.
[55] S. Vadivel, M. Vanitha, A. Muthukrishnaraj, N.J. Balasubramanian, Graphene oxide–BiOBr composite material as highly efficient photocatalyst for degradation of methylene blue and rhodamine-B dyes, J. Water. Process. Eng. 1 (2014) 17–26, https://doi.org/10.1016/j.jwpe.2014.02.003.
[56] M. Hassanpour, H. Safardoust-Hojaghan, M.J. Salavati-Niasari, Degradation of methylene blue and Rhodamine B as water pollutants via green synthesized Co3O4/ZnO nanocomposite, J. Mol. Liq. 229 (2017) 293–299, https://doi.org/10.1016/j.molliq.2016.12.090.
[57] Y. Na, Y.-I. Kim, D.W. Cho, D. Pradhan, Y.J. Sohn, Adsorption/photocatalytic performances of hierarchical flowerlike BiOBrxCl1 − x nanostructures for methyl orange, Rhodamine B and methylene blue, Mat. Sci. Semicon. Proc. 27 (2014) 181–190, https://doi.org/10.1016/j.mssp.2014.06.043.
[58] M. Ahmad, E. Ahmed, Z. Hong, W. Ahmed, A. Elhissi, N. Khalid, Photocatalytic, sonocatalytic and sonophotocatalytic degradation of Rhodamine B using ZnO/CNTs composites photocatalysts, Ultrason. Sonochem. 21 (2) (2014) 761–773, https://doi.org/10.1016/j.ultsonch.2013.08.014.
[59] Z. Chen, T.-T. Fan, X. Yu, Q.-L. Wu, Q.-H. Zhu, L.-Z. Zhang, J.-H. Li, W.-P. Fang, X.-D.J. Yi, Gradual carbon doping of graphitic carbon nitride towards metal-free visible light photocatalytic hydrogen evolution, J. Mater. Chem. A 6 (31) (2018) 15310–15319, https://doi.org/10.1039/C8TA03303J.
[60] V.Z. Baldissarelli, T. de Souza, L. Andrade, L.F.C. de Oliveira, H.J. José, R. de Fátima Peralta Muniz Moreira, Preparation and photocatalytic activity of TiO2-exfoliated graphite oxide composite using an ecofriendly graphite oxidation method, Appl. Surf. Sci. 359 (2015) 868–874, https://doi.org/10.1016/j.apsusc.2015.10.199.
[61] T. Peng, J. Zhang, S. Ray, H. Fakhouri, X. Xu, F. Arefi-Khonsari, J.A. Lalman, Enhanced TiO 2 nanorods photocatalysts with partially reduced graphene oxide for degrading aqueous hazardous pollutants, Environ. Sci. Pollut. Res. 25 (18) (2018) 17553–17564, https://doi.org/10.1007/s11356-018-1886-5.
[62] R. Tabit, O. Amadine, Y. Essamlali, K. Dânoun, A. Rhihil, M. Zahouily, Magnetic CoFe 2 O 4 nanoparticles supported on graphene oxide (CoFe 2 O 4/GO) with high catalytic activity for peroxymonosulfate activation and degradation of rhodamine B, RSC Adv. 8 (3) (2018) 1351–1360, https://doi.org/10.1039/C7RA09949E.
[63] X. Wei, N. Li, X. Zhang, Cu@ C nanoporous composites containing little copper oxides derived from dimethyl imidazole modified MOF199 as electrocatalysts for hydrogen evolution reaction, Appl. Surf. Sci. 425 (2017) 663–673, https://doi.org/10.1016/j.apsusc.2017.07.067.
[64] Y. Wong, Y. Szeto, W. Cheung, G. McKay, Equilibrium studies for acid dye adsorption onto chitosan, Langmuir 19 (19) (2003) 7888–7894, https://doi.org/10.1021/la030064y.
[65] K. Yu, S. Yang, C. Liu, H. Chen, H. Li, C. Sun, S.A. Boyd, Degradation of organic dyes via bismuth silver oxide initiated direct oxidation coupled with sodium bismuthate based visible light photocatalysis, Environ. Sci. Technol. 46 (13) (2012) 7318–7326, https://doi.org/10.1021/es3001954.
[66] W. Zhang, C. Zhou, W. Zhou, A. Lei, Q. Zhang, Q. Wan, B. Zou, Fast and considerable adsorption of methylene blue dye onto graphene oxide, Bull. Environ. Contam. Toxicol. 87 (1) (2011) 86, https://doi.org/10.1007/s00128-011-0304-1.